*Journal of Structural Chemistry, Vol. 47, Supplement, pp. S141-S150, 2006*


# MELTING AND HOMOGENEOUS CRYSTALLIZATION OF A LENNARD-JONES SYSTEM

**A. V. Kim[1] and N. N. Medvedev[2]**

UDC 532.74

Melting and homogeneous crystallization in a Lennard-Jones system of 10,976 atoms in a model box with periodic boundary conditions were investigated by the molecular dynamics method in an *NVE* ensemble. Crystal melting occurs by arbitrary generation and growth of local defects transformed into regions of a disordered phase. These defects gradually span the entire space of the sample, absorbing the residual islands of crystal. Homogeneous crystallization of a liquid starts with generation of crystal nuclei which grow into defective crystals. The resulting crystal varies in structure between different realizations of the model. Face-centered cubic (fcc) structures prevail. A hexagonal close packing (hcp) structure is present on the boundaries of fcc regions and arises from disordering in alternation of atomic planes. Multiple twinning of the fcc structure is observed, and aggregates with fivefold symmetry have been found.

**Keywords:** molecular dynamics, liquid structure, Voronoi–Delaunay method, melting, homogeneous crystallization, fivefold symmetry.

## INTRODUCTION

Systems of Lennard-Jones atoms are generally used as models for investigating fundamental processes during phase transitions in simple (monoatomic) liquids. Melting and crystallization have long been under study, but many details of the ensuing structural changes are not clear as yet. For these studies we need computer models that make it possible to trace the position of each atom. The models should be large enough, at least larger than typical structural inhomogeneities arising from a phase transition. Modern computer technology and computer simulation methods permit researchers to create models on which they can trace not only changes in thermodynamic parameters, but also subtle features of structural rearrangements in the sample.

Structural analysis is performed using the Voronoi–Delaunay method [1]. In this work we restricted ourselves to the use of Delaunay simplices. A Delaunay simplex is a quadruple of adjacent atoms. For disordered and thermally perturbed systems, simplices are distorted tetrahedra. Using a quantitative measure of the simplex form [1, 2], we isolate those simplices that approach an ideal tetrahedron in shape and employ them for structural analysis of our models. These are just the kind of simplex typical for a dense crystal structure. They also occur in liquids, but their mutual arrangement differs radically from that in crystals.

To model a liquid–solid phase transition one often employs an *NPT* ensemble; i.e., the number of particles, as well as the pressure and temperature of the sample, are kept constant [3-5]. Indeed, in real experiment, physical processes generally occur in "ambient" conditions (constant pressure and temperature). *NVT* is another widely used thermodynamic

[1]Novosibirsk State University. [2]Institute of Chemical Kinetics and Combustion, Siberian Division, Russian Academy of Sciences, Novosibirsk; nikmed@kinetics.nsc.ru. Translated from *Zhurnal Strukturnoi Khimii*, Vol. 47, Supplement, pp. S144-S153. Original article submitted April 12, 2006.

ensemble, in which volume (mean density) of the sample is kept constant instead of pressure. The most popular ensemble used for molecular dynamic simulations is *NVE*, where the total energy of the system is maintained at a constant level. This ensemble is useful in many fields of applied research where inclusion of thermodynamic details is not critical. It embodies a classical conservative mechanical system and does not need any special techniques as those needed for realization of statistical ensembles. In the latter case, pressure or temperature are to be kept constant, which is achieved by scaling the atomic velocities and the dimensions of the model box [4-7]. The *NVE* ensemble is more suitable for studies of processes that occur at atomic levels and within short periods of time. For example, spontaneous generation of crystallization nuclei significantly lowers the local temperature (kinetic energy) of atoms in the vicinity of the nucleus. Setup of thermodynamic equilibrium at this site is not an instant process; therefore, such processes are preferably studied under adiabatic, but not isothermal conditions.

In this work, we developed a molecular dynamic program for the *NVE* ensemble, specially designed for work with large models. Some special techniques were used to accelerate program operation with models of large numbers of atoms. The idea of linked lists allows fast enumeration of the nearest neighbors during calculation of atomic interactions with the environment [4]. This program was used to simulate melting and crystallization of a Lennard-Jones system of 10,976 atoms. Variation of temperature (kinetic energy) and structure during the phase transition has been studied. The results of this work provide better insight into the mechanisms of melting and crystallization at the atomic level.

## PROCEDURE

In the molecular dynamics (MD) method, we solve Newton's system of equations. For this we use Verlet's algorithm, which is accurate enough and simple to use [7]. For the interatomic interaction potential we take the Lennard-Jones potential $U(r) = 4\varepsilon[(\sigma/r)^{12} - (\sigma/r)^6]$, where $r$ is the distance between atoms; $\varepsilon$ is the depth of the potential well; and $\sigma$ is the size of the "rigid nucleus" of the atom. The values of the parameters used are those of argon:

$$T^* = \varepsilon/k_B = 119.8 \text{ K}, \sigma = 3.405 \cdot 10^{-10} \text{ m}.$$

Calculations were fulfilled with reduced $\varepsilon$ units for energy and $\sigma$ for distance. The trimming radius of the potential $r_{cut}$ was chosen equal to $3\sigma$. The ensuing abrupt change in the potential at the point $r_{cut}$ was smoothed by adding a linear function.

The linked list technique was used to accelerate program operation for large models [4] to achieve higher efficiency $O(N)$ of the algorithm. The run time grows as a linear function with the number of atoms in the model. For the standard algorithm, we are bound to enumerate all atoms of the system every time we calculate the force acting on an atom; in this case, the efficiency was estimated as $O(N^2)$.

The model box was divided into relatively small cells, numerated in terms of their coordinates. This makes it possible to immediately calculate the number of the cell with the given point from the coordinates of this (arbitrary) point within the box. Each cell was assigned the indices of its constituent atoms. Thus when calculating the force acting on the given atom, one can avoid enumerating all atoms of the system.

Indeed, from the coordinates of the atom one can immediately calculate the number of the cell where it lies; from the number of the latter (and from the numbers of adjacent cells) one can immediately determine (using lists of atoms assigned to the cells) the atoms of the nearest environment of the given atom.

The size of the cells obtained by dividing the box is to be chosen approximately equal to volume per atom:

$$l_{cell} = k\sqrt[3]{\frac{V_{box}}{N}}.$$

The cell size affects the efficiency of the algorithm. We investigated the dependence of the computing time of the potential energy of the system on the coefficient $k$. The dependence is a function with a minimum at approximately $k = 2$. This value of the coefficient was chosen for further calculations.

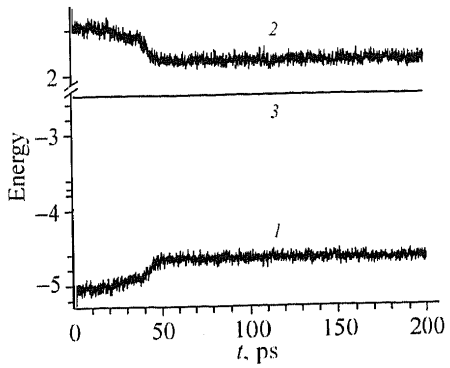


**Fig. 1.** Behavior of the potential (*1*), kinetic (*2*), and total (*3*) energies during fcc crystal melting.

Below we compare the computing times of the total energy for models with different numbers of atoms using the standard algorithm and ours. While for 500 atoms both algorithms show approximately the same time, for 32,000 atoms the difference is significant. All computations were performed on a PC with an Athlon processor, 1.82 GHz. Evolution of a system of 10,976 atoms within 1 ns takes approximately 36 h computer time.

| Model energy calculation time | 500 atoms | 4000 atoms | 32,000 atoms |
|---|---|---|---|
| Enumeration of all atoms | 0.2 s | 0.75 s | 62.9 s |
| Linked lists | 0.2 s | 0.2 s | 1.7 s |

The integration step $\Delta t$ is an important parameter of calculations. Large steps lead to a significant error in solving equations by numerical methods, while small steps leads to unreasonably long simulation times. We chose $\Delta t = 0.005$ as an optimal value, which corresponds to 0.01 ps. Figure 1 illustrates conservation of energy in the case of our program. A test system was an overheated fcc crystal, which melted and became an equilibrium liquid.

Since crystal melting leads to structure disordering, the potential energy increases, while the kinetic energy decreases. The total energy will not change. Our calculations show that the total energy of the system is conserved. In Fig. 1, the curve of the total energy (curve *3*) is shown as a horizontal straight line. Pronounced "noise" on curves *1* and *2* implies fluctuations of potential and kinetic energies in the course of molecular dynamic evolution. These fluctuations, however, occur under conditions of the preserved total energy of the system.

## MELTING

**Melting of a dense fcc crystal.** In the initial configuration of a model dense crystal, atoms lie at the sites of the fcc lattice where the shortest interatomic distance (lattice parameter) is $\sqrt[6]{2}\sigma$, which corresponds to a minimum of the Lennard-Jones potential. The crystal was heated in a stepwise procedure (Fig. 2). In the first step, all atoms acquired random (in magnitude and direction) velocities, which were normalized in such a way that the kinetic energy corresponded to the given temperature (in the first step, $T = 1$ in $\varepsilon/k_B$ units). Redistribution between the kinetic and potential energies takes place within the first 50 steps (0.5 ps) (fast relaxation; Fig. 2, insert). Then relaxation continued for another 10,000 steps, which corresponds to ~0.1 ns (Fig. 2, region *1*).

In the second step, the sample was quickly heated to $T = 1.2$. Relaxation set the temperature to 0.9 (Fig. 2, region *2*). This stepwise heating led to a temperature of 1.6 at which the sample spontaneously melted after ~0.1 ns (Fig. 2, region *5*). In our ensemble, melting is accompanied by a decrease in the kinetic energy and an increase in the potential energy. The sample temperature lowered to $1.32\varepsilon/k_B$.

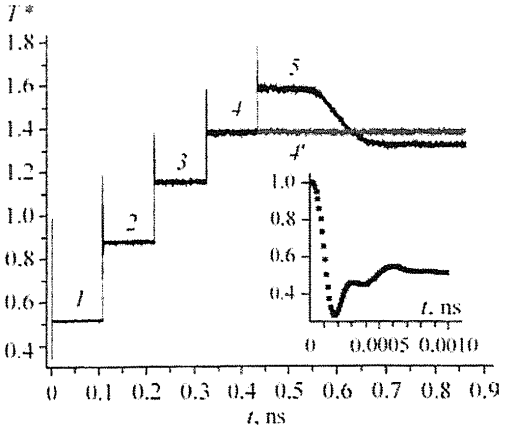


**Fig. 2.** Stepwise heating and melting of an fcc crystal containing 10,976 atoms. Insert: fast relaxation of the system after instant heating of the sample.

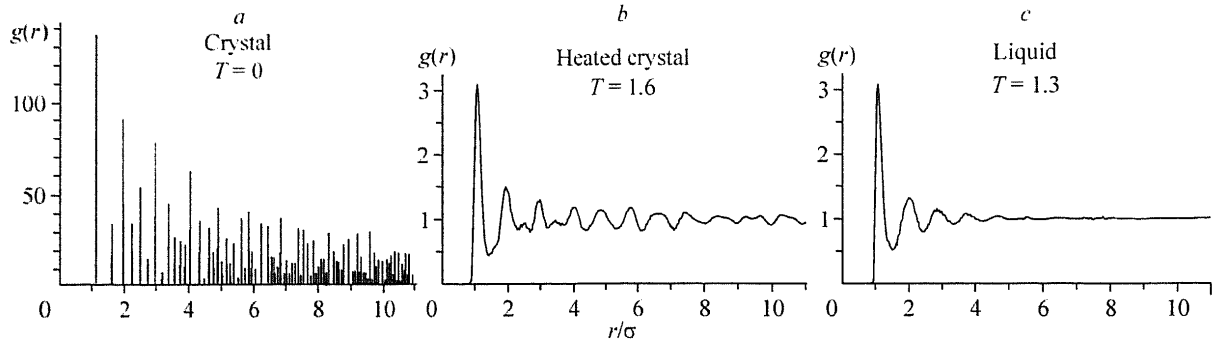


**Fig. 3.** Radial distribution function of an fcc crystal at $T = 0$ (*a*), of a crystal heated to $T = 1.6$ (*b*), after melting (*c*).

The temperature of the resulting liquid ($T = 1.32$) proved to be lower than the crystal temperature in the previous heating step ($T = 1.4\varepsilon/k_B$). Continuous relaxation of the crystal at $T = 1.4$, however, did not lead to melting (Fig. 2, curve *4'*). This indicates that after minor overheating the crystal remains stable enough.

The radial distribution functions (RDFs) calculated for this model reveal the ensuing structural changes (Fig. 3). During heating the sharp peaks of the RDF of the crystal structure (Fig. 3*a*) become diffuse, but long-range order is well visible even at $T = 1.6$ as long as the sample remains crystalline (Fig. 3*b*). In liquid, long-range order vanishes, and the oscillations of the radial function decay quickly with distance (Fig. 3*c*).

**Melting of a loose fcc crystal.** Since we work with the *NVE* ensemble, the average density does not change after melting. The liquid obtained after melting of a dense crystal has exaggerated density and corresponds to a state at a high pressure. To obtain a model liquid with normal density we took a crystalline sample with a density of a liquid phase, $\rho = 0.85$ (the density of the triple point for a Lennard-Jones liquid). For the initial configuration we again took an fcc crystal, but this time the interatomic distance was $1.056\sigma$. The sample was heated as described above, i.e., instant heating (by $\sim 0.25\varepsilon/k_B$) with further relaxation of the system. Melting in this case occurred at a temperature of ~0.6. Figure 4 shows only the melting step.

The radial distribution functions calculated for this model are similar to those shown in Fig. 3. The system has long-range order until the kinetic energy is "pumped" into potential energy; this can be seen from the peaks on the RDF in the region of minor values of $r$. After a new equilibrium between the kinetic and potential has set in, the crystal structure vanishes completely, and the system is a liquid with typical quick damping of the RDF.

Details of the inner structure of the sample may be presented using the Voronoi–Delaunay method. To visualize the

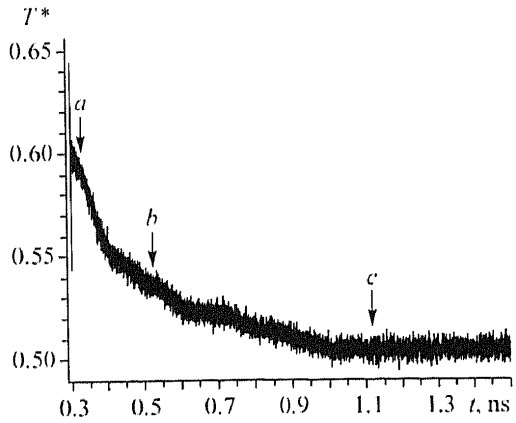


**Fig. 4.** Melting of an fcc crystal with density 0.85. The arrows mark the structures shown in Fig. 5.

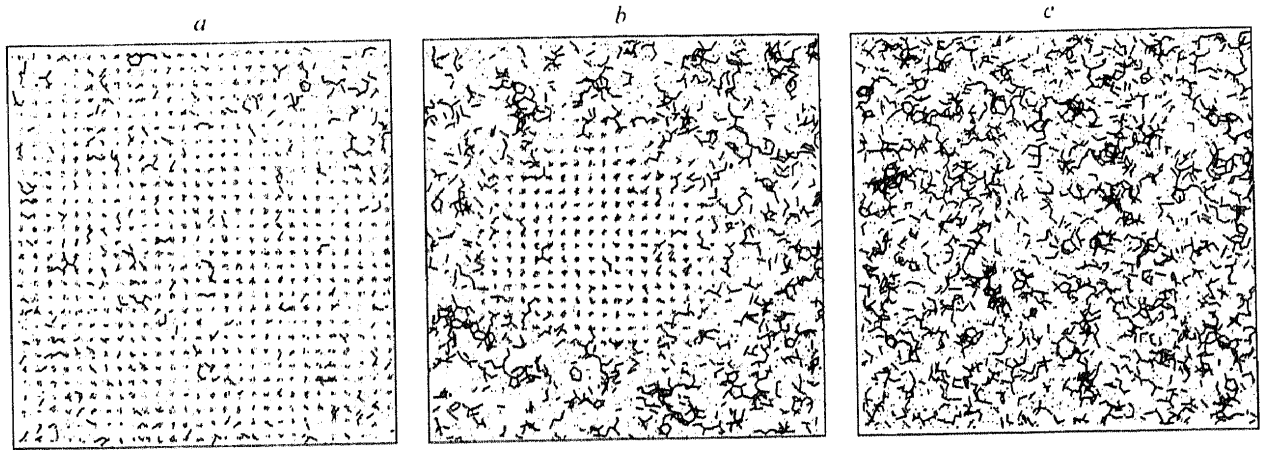


**Fig. 5.** Melting of an fcc crystal. The points denote the centers of simplices shaped like a regular tetrahedron. The segments imply that adjacent tetrahedral simplices have a common face. The pictures correspond to configurations taken at the moments shown by arrows in Fig. 4. Rows of isolated points denote an fcc structure. Disordered clusters of segments are inherent in liquids.

structure we draw the centers of the simplices shaped like good tetrahedra [1, 2]. If good tetrahedra share faces, their centers are linked by a line. In this approach, the ideal fcc crystal corresponds to series of isolated points [8, 9] (in hcp structures, tetrahedra contact only by their edges). In the course of heating, the even rows of simplices are broken, and clusters of tetrahedral simplices not typical of hcp structures, in particular, face-sharing tetrahedra appear in the model (Fig. 5*a*). Then the local defects are gradually accumulated and grow, merging into a single disordered region. Islands of crystal still remain in the model (Fig. 5*b*), but they quickly vanish, resulting in a uniform liquid phase (Fig. 5*c*). The character of melting is the same for both dense and loose crystals.

## CRYSTALLIZATION

To study crystallization we cooled the above model of a liquid phase with density 0.85. Cooling was a stepwise procedure similar to crystal heating (Fig. 2). The kinetic energy decreased immediately (by a quantity corresponding to a decrease of 0.1 in temperature); after that, system relaxation took place (Fig. 6, regions I-IV). Cooling was continued until a structural rearrangement started in the sample which is clearly seen from the sharp growth of kinetic energy in region IV at a temperature of 0.32.

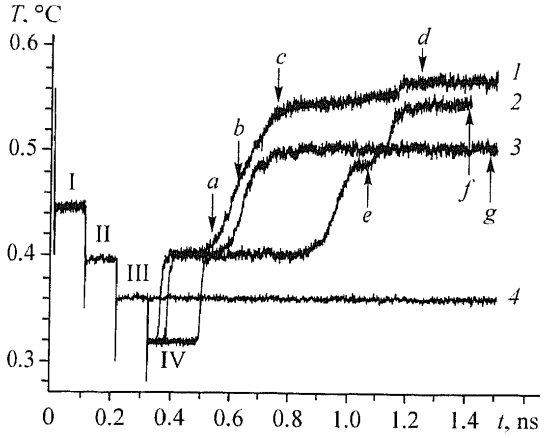


**Fig. 6.** Time dependence of the sample temperature during simulation of crystallization. In the range from 0 ns to 0.32 ns (regions I-III) the liquid undergoes stepwise cooling. Curves *1-3* show different routes of crystallization from the same configuration of the model from region IV. Curve *4* demonstrates that an overcooled disordered phase exists at a temperature exceeding the temperature of the start of the structural rearrangement.

In contrast to melting, during which the crystal is transformed into a disordered uniform phase, crystallization gives rise to various structures. This is understandable because the form of crystal nuclei and the character and spatial arrangement of defects may be rather specific. To examine this problem we considered several models of crystallized liquid obtained under identical conditions. The initial configuration of the liquid with given kinetic energy was the same, but the initial directions of the velocities of atoms were set random. The behavior of three such models is depicted in Fig. 6 (curves *1-3*). One can immediately see that structural rearrangement in these models (growth of kinetic energy) starts at different moments of time. All models have one feature in common: the first step of structure modification ends at $T = 0.4$. Within a certain period of time thereafter, the system undergoes steady evolution. As shown by our analysis, a liquid with a density of 0.85 overcooled to a temperature of 0.32 is initially transformed into a denser disordered state, and then starts to undergo crystallization proper. Since the model cube does not change in volume, a compact void (bubble) with a diameter of a few $\sigma$ appears after a disordered dense phase has formed at $T = 0.4$. This void, however, occupies minor volume than the model box and does not hinder observation of further structural rearrangements in the system.

Figure 7*a-d* shows the structure of configurations of model 1 at different moments of time (shown by arrows in Fig. 6, curve *1*). As in Fig. 5, points inside the model box represent the centers of Delaunay simplices that are good tetrahedra, and the lines connect the centers of these simplices if they have a common face. Figure 7*a* has a region of isolated points corresponding to crystal nucleation. Once formed, a crystal nucleus starts to grow quickly (which can be seen from fast growth of kinetic energy), and after 0.1 ns the crystal phase occupies half of the sample (Fig. 7*b*); after another 0.15 ns it fills the whole sample, but still has many defects (Fig. 7*c*). Then the kinetic energy does not change so quickly, and no drastic rearrangements seem to take place, while defects gradually vanish from the structure. Nevertheless, this is not a uniform process. At a moment of time marked by arrow *d* on curve *1* (Fig. 6), the curve shows a minor (but drastic) change in the kinetic energy of the sample, resulting in elimination of many defects and higher quality of the crystal structure (Fig. 7*d*).

The observed rows of short segments correspond to rows of face-sharing pairs of tetrahedra. These pairs (trigonal bipyramids) are characteristic elements of hcp structures. Possible appearance of layers of an hcp structure within the fcc structure is a well-known fact. This is the result of alternation of crystal faces. The order of alternation is represented as

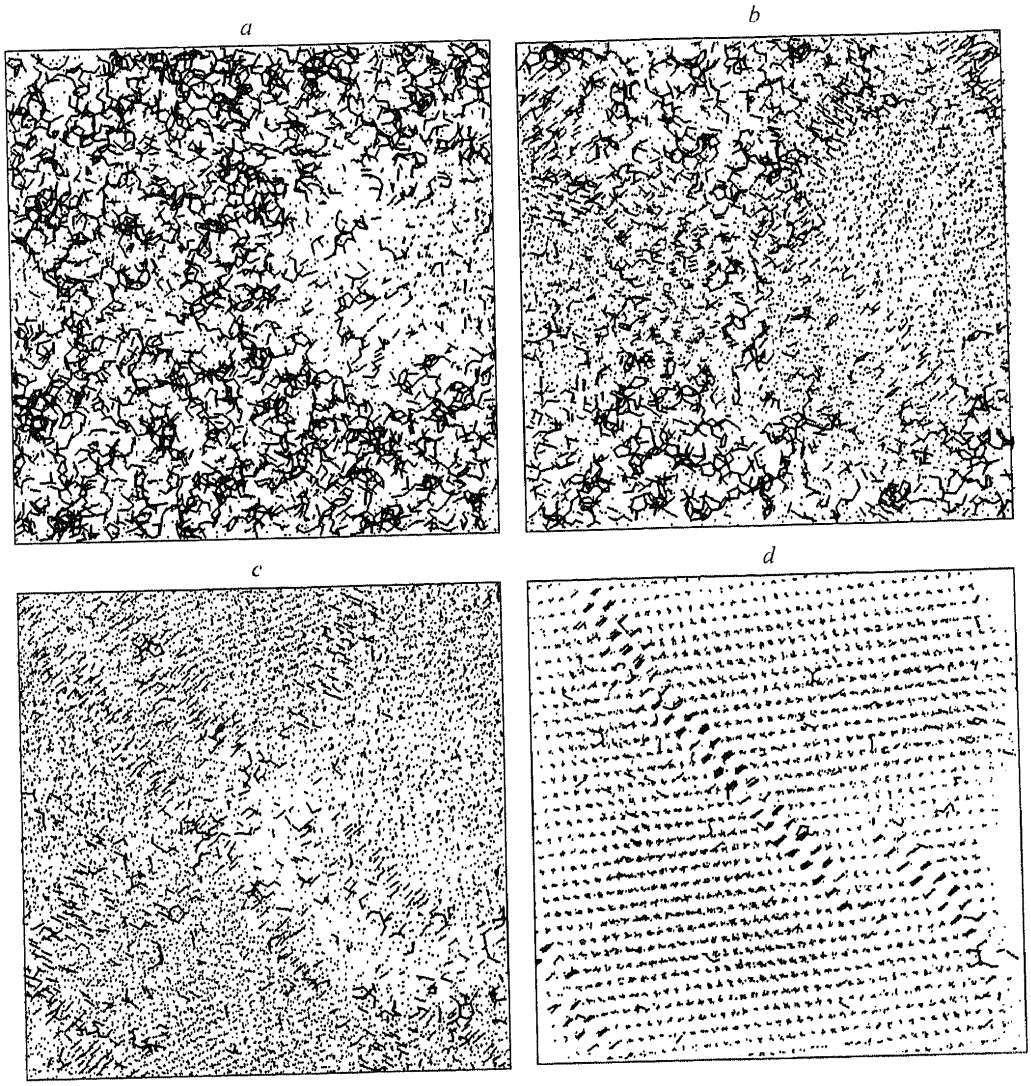


**Fig. 7.** Nucleation and growth of crystal in model 1 (Fig. 6, curve *1*). Structures *a*, *b*, *c*, and *d* correspond to moments of time shown by lettered arrows in Fig. 6. The arrangement of good tetrahedral simplices inside the model box is shown (see text). Rows of short segments correspond to layers of the hcp structure.

*ABCABC*... for fcc crystals and *ABAB*... for hcp crystals. The sequence may be *ABCABABABC* with sections inherent in hcp structures if the normal sequence is violated.

The resulting picture of crystallization is generally approximately the same for all models in question. An hcp structure is the basic crystal structure. However, it always has defects; the basic type of defect is violated alternation of crystal planes, leading to layers of hcp structure [8, 9]. The particular arrangement of defects in a model, however, is unpredictable.

In the course of crystallization, nontrivial structural transformations can take place. An interesting example is furnished by model 2 (Fig. 6, curve *2*). At a moment of time marked by arrow *e* in Fig. 6 during crystallization, structures with fivefold symmetry appeared. In Fig. 8*e* they can be seen as stacks of five-membered rings. Stacks of this kind were previously observed in models of hard sphere packings with crystalline nuclei [2].

The resulting structure was relatively stable; its lifetime was 0.1 ns. Then crystallization continued, resulting in a normal crystal phase with familiar defects at a moment of time labeled by arrow *f* in Fig. 6 (Fig. 8*f*).

In our approach, the five-membered ring means a closed aggregate of five good tetrahedra. This structure (pentagonal bipyramid of seven atoms) is well known for dense monoatomic systems and sphere packings [10-12] (Fig. 9*a*).

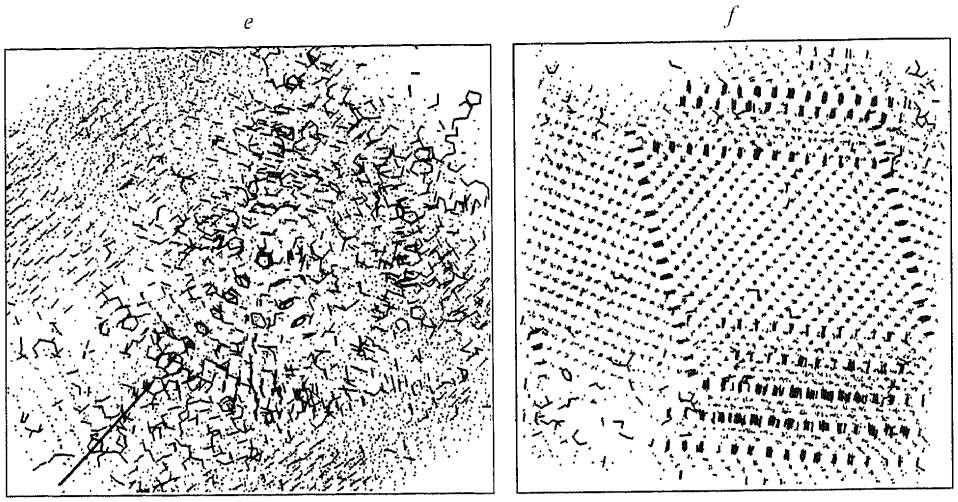


**Fig. 8.** Crystallization of model 2 (Fig. 6, curve *2*). Structures *e* and *f* correspond to the moments of time indicated in Fig. 6. In configuration *e*, one can see stacks of five-membered rings, which point to the existence of structures with fivefold symmetry axis (shown by an arrow). In configuration *f*, structures of this kind are absent.

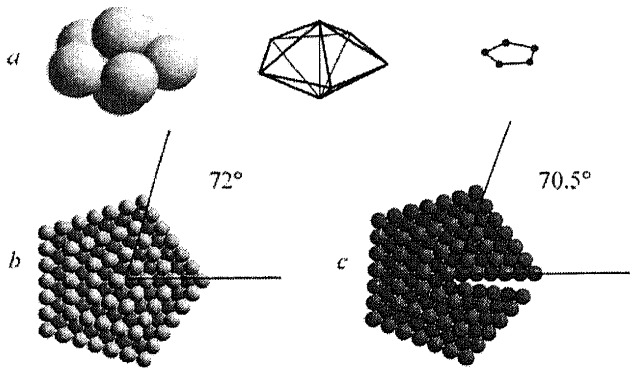


**Fig. 9.** Nature of structures formed by spherical atoms and having a fivefold symmetry axis: *a* — decahedron–pentagonal bipyramid (ring of five nearly perfect tetrahedra). In terms of the Voronoi–Delaunay method the bipyramid is represented by a five-membered ring, see text; *b* — the Bagley structure fills the entire space in a uniform manner; *c* — fivefold twin of fcc; in the case of a perfect fcc structure, it has a gap of 7.5.

This is part of the icosahedral stacking of atoms. Icosahedra, however, are typical for small atomic clusters alone and are not met in bulk samples. Three-dimensional disordered close packings of spheric atoms (in systems with periodic boundary conditions) typically have separate pentagonal bipyramids [1, 10, 12, 13], and crystallization can form stacks of these configurations — polydecahedra [2]. A stack of this kind is the "axis" of the pentagonal prism. The possibility for pentagonal prisms to exist in packings of spheric atoms was examined in detail in crystallographic works [11, 14-16]. So-called Bagley structures are possible. A Bagley structure has one fivefold axis and fills space in a uniform way [11, 17, 18]. Each sector of the prism has a crystal structure that differs slightly from closest packings (orthorhombic body-centered structure with density 0.7236 [11]); at the boundaries of the sectors, changed alternation of crystal planes leads to "rotation" of this structure through an angle equal to one fifth of the total angle: $2\pi/5$ (Fig. 9*b*).

As the pentagonal prism increases in size, the crystal structure becomes an hcp structure (in its sectors), which is more stable. In crystallography, this is generally considered to be a fivefold twin of the fcc structure, especially because the

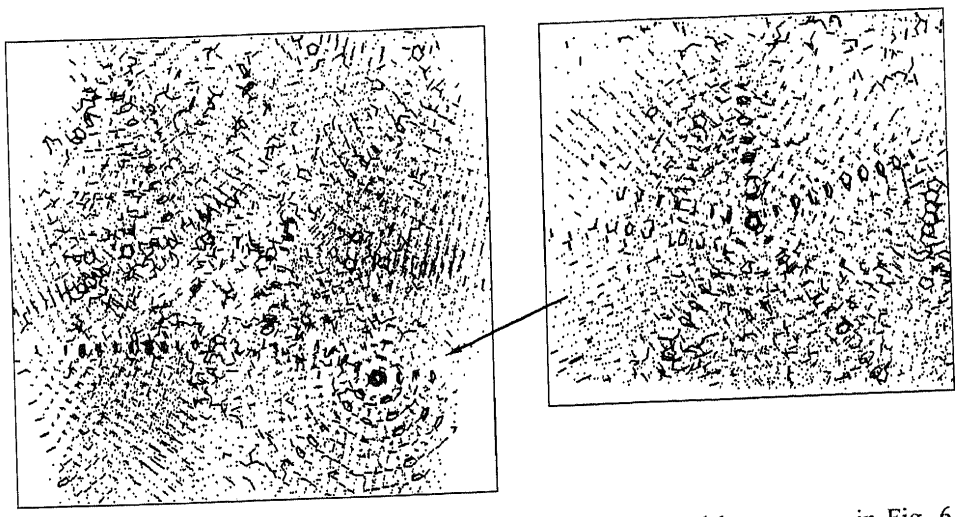

**Fig. 10**. Structure of model 3. The moment of time indicated by arrow *g* in Fig. 6. Right: fragment of this model that demonstrates an aggregate with a fivefold axis (scaled-up).

latter typically has macroregions of regular tetrahedral form, which may be arranged in a ring. Here we have another problem: the dihedral angle of the ideal tetrahedron is ~70.5°, i.e., slightly smaller than one fifth of the total angle and the fivefold twin of the fcc crystal, therefore, has a gap of 7.5° (Fig. 9*c*). In (physical or computer) experiment, where atoms are perturbed by thermal motions, the gap readily diffuses, and the nature of the pentagonal prism (whether this is a Bagley structure or a fivefold fcc twin) is not a critical issue.

Model 3 (curve *3*, Fig. 6) demonstrates that a more stable structure with fivefold symmetry is formed compared to the structure of model 2. In addition to isolated stacks of five-membered rings here we have a large fragment with a fivefold symmetry axis (Fig. 10). As a result, our molecular dynamic experiment did not lead to a uniform crystal during run time; instead, it gave separate nuclei with different orientations. The potential energy of this system is certainly higher than that in a uniform fcc crystal, which accounts for the lower kinetic energy of this model compared to models 1 and 2 (Fig. 6).

## CONCLUSIONS

Thus we have studied melting and homogeneous crystallization of Lennard-Jones systems using the molecular dynamics method in the *NVE* ensemble. We have designed a special program in which the computing time increases as a linear function with the number of atoms in the model ($O(N)$), while for many accessible programs their efficiency increases as a quadratic dependence with time ($O(N^2)$). This is critical for the given problem. First, our models should be large enough, namely, they should exceed the typical size of structural inhomogeneities arising during melting and crystallization. Moreover, melting and crystallization occur within relatively long periods of time, and the rate of program operation is a critical factor.

We work with a Lennard-Jones system containing 10,976 atoms in a model box with periodic boundary conditions. Calculation was performed for times of up to 1.6 ns. It has been shown that local defects initially form during crystal melting; these defects grow into regions of a disordered phase (liquid). They gradually fill the entire volume of the sample, absorbing the residual islands of the crystal phase. Similarly, crystallization of a liquid starts with formation of crystal nuclei, which grow into defective crystal. The particular structure of the resulting crystal differs between realizations of the same model. Nevertheless, the fcc structure prevails. Regions with hcp structure are mainly present on the boundaries of fcc regions; they are the consequence of broken order of alternation of atomic planes. In addition to the ordinary crystal nuclei crystallization forms structures with a fivefold symmetry axis — pentagonal prisms, which can be interpreted as fivefold "twins" of the fcc structure.

This work was supported by RFBR grant No. 05-01-32647.

## REFERENCES


1. N. N. Medvedev, *Voronoi–Delaunay Method in Structural Studies of Noncrystalline Systems* [in Russian], Siberian Division, Russian Academy of Sciences, Novosibirsk (2000).
2. N. N. Medvedev, A. Bezrukov, and D. Shtoyan, *Zh. Strukt. Khim.*, **45**, 24-31 (2004).
3. Yu. K. Tovbin (ed.), *Molecular Dynamics Method in Physical Chemistry* [in Russian], Nauka, Moscow (1996).
4. M. P. Allen and D. J. Tildesley, *Computer Simulation of Liquids*, Clarendon Press, Oxford (1987).
5. D. Frenkel and B. Smit, *Understanding Molecular Simulation: From Algorithm to Applications*, Academic Press, San Diego USA (1996).
6. J. M. Haile, *Molecular Dynamics Simulation: Elementary Methods*, Wiley, New York (1997).
7. L. Verlet, *Phys. Rev.*, **159**, 98-103 (1967); *ibid.*, **165**, 201-214 (1968).
8. M. G. Alinchenko and N. N. Medvedev, *Using Voronoi–Delaunay Method for Investigating Structural Defects in Crystals, Proceedings of the 10th Russian Conference* "Structure and Properties of Metallic Melts and Melted Slags," Vol. 1, South Urals State University, Chelyabinsk (2001), pp. 19-23.
9. N. N. Medvedev, *Physica*, **A314**, 678-685 (2002).
10. J. D. Bernal, *Proc. R. Soc. Lond.*, **A280**, 299-322 (1964).
11. B. G. Bagley, *Nature*, **208**, 674/675 (1965).
12. F. Spaepen, *ibid.*, **408**, 781-785 (2000).
13. B. O'Malley and I. Snook, *Phys. Rev. Lett.*, **90(8)**, 085702 (2003).
14. H. Hofmeister, *Cryst. Res. Technol.*, **33**, 3-25 (1998).
15. V. G. Grysnov, J. Heydenreich, A. M. Kaprelov, et al., *ibid.*, **34**, 1091-1119 (1999).
16. N. A. Bulienkov and D. L. Tytik, *Izv. Akad. Nauk, Ser. Khim.*, No. 1, 1-19 (2001).
17. B. G. Bagley, *J. Cryst. Growth*, **6**, 323-326 (1970).
18. C. Kittel, *Introduction to Solid State Physics*, Wiley, New York (1996).